Small bandgap bowing in $In_{1-x}Ga_xN$ alloys

J. Wu,
Applied Science and Technology Graduate Group, University of California, Berkeley,
and Materials Sciences Division, Lawrence Berkeley National Laboratory,
Berkeley, CA 94720,
W. Walukiewicz, K.M. Yu, J.W. Ager III,
Materials Sciences Division, Lawrence Berkeley National Laboratory,
Berkeley, CA 94720,
E.E. Haller,
Department of Materials Science and Engineering, University of California, Berkeley,
and Materials Sciences Division, Lawrence Berkeley National Laboratory,
Berkeley, California 94720,
Hai Lu, and William J. Schaff
Department of Electrical and Computer Engineering, Cornell University, Ithaca, NY
14853

High-quality wurtzite-structured In-rich $In_{1-x}Ga_xN$ films ($0 \le x \le 0.5$) have been grown on sapphire substrates by molecular-beam epitaxy. Their optical properties were characterized by optical absorption and photoluminescence spectroscopy. The investigation reveals that the narrow fundamental bandgap for InN is near 0.8eV and that the bandgap increases with increasing Ga content. Combined with previously reported results on the Ga-rich side, the bandgap versus composition plot for $In_{1-x}Ga_xN$ alloys is well fit with a bowing parameter of ~ 1.4 eV. The direct bandgap of the $In_{1-x}Ga_xN$ system covers a very broad spectral region ranging from near-infrared to near-ultraviolet.

PACS numbers: 78.66.Fd, 72.80.Ey
Electronic Mail: w_walukiewicz@lbl.gov, jqwu@ux8.lbl.gov

The $In_{1-x}Ga_xN$ alloy system has been studied extensively in recent years. An especially intense effort has been directed towards the studies of Ga-rich alloys, which are used as the active layer in blue and green light emitting diodes and lasers [1-4]. Another attribute of this alloy system is that the energy gap can be varied in a wide spectral range. For example, it has been shown that the bandgap can be decreased from the GaN value, 3.4 eV, down to ~2.3 eV for $In_{0.4}Ga_{0.6}N$ [5-8]. Studies of the optical properties of these Ga-rich alloys have shown a strong dependence of the fundamental bandgap on the alloy composition. When a bandgap of ~ 1.9 eV for InN is assumed as the end point value, large bowing parameters are required to fit the composition dependence of the fundamental bandgap energy. For example, a bowing parameter of 2.5 eV was obtained from optical absorption measurements and a value of 4.4 eV was obtained from the location of the emission peaks [5]. The bandgap value of ~ 1.9eV for InN was determined in early studies mainly by interband optical absorptions performed on InN thin films deposited by sputtering techniques [9-10] and metalorganic vapor phase epitaxy [11]. The electron concentration in those films was usually over 10^{20} cm^{-3} and the room-temperature mobility was below 100 cm^2/Vs. Despite extensive efforts, no reliable light emission associated with an energy gap near 1.9 eV has ever been reported in these early studies of InN.

Recent progress in epitaxial growth techniques has led to the availability of InN crystals with considerably lower electron concentrations and much higher electron mobilities. Films with electron concentrations in the low 10^{18} cm^{-3} range with room temperature mobilities well in excess of 1300 cm^2/Vs in InN have been grown by molecular beam epitaxy [12-15]. It has been reported very recently that these improved InN films show intense photoluminescence (PL) at energies around 0.8 eV at room temperature [14-16]. Along with the strong PL, a clear absorption edge [14-16] and a photo-modulated reflectance transition feature have also been observed at this energy [16]. Thus, the fundamental bandgap of InN has been determined to be near 0.8 eV [15-16].

In this paper, we report our systematic study on the optical properties of In-rich $In_{1-x}Ga_xN$ alloys grown by improved epitaxial method. It was found that these alloys

show strong infrared PL signal, as expected from an InN bandgap of ~ 0.8 eV. The emission spectrum of the $In_{1-x}Ga_xN$ system thus extends to near infrared. The bowing parameter in the entire composition range can be fit with a small bowing parameter of ~ 1.4 eV.

$In_{1-x}Ga_xN$ films (~240 nm) were grown on (0001) sapphire with an AlN buffer layer (~200 nm) by molecular beam epitaxy [13]. The growth temperature is in the range of 470 ^oC to 570 ^oC. The Ga atomic fraction was determined by X-ray diffraction (XRD) assuming a complete lattice relaxation. The XRD analysis shows that high-quality wurtzite-structured $In_{1-x}Ga_xN$ epitaxial layers formed with their c-axis perpendicular to the substrate surface. The samples were characterized by conventional optical absorption (abs) and photoluminescence spectroscopy. The optical absorption measurements were performed on a CARY-2390 NIR-VIS-UV spectrophotometer. The PL signals were generated in the backscattering geometry by excitation with the 476.5 nm line of an argon laser. The signals were then dispersed by a 1 m double-grating monochromator and detected by a Ge photodiode.

The samples exhibit strong infrared PL signal even at room temperature. Figure 1(a) shows the PL signals for samples with a wide range of Ga compositions from 0 to 0.5. Both room temperature (295K) and low temperature (11K) results are shown. As expected, the PL peak energy shows a strong blueshift from the bandgap of InN (0.77 eV at room temperature) with increasing Ga content. The linewidth of the PL peak is significantly broadened as x increases. The temperature also has an interesting effect on the PL signal, which will be discussed below.

Figure 1(b) shows the absorption coefficient squared plotted as a function of photon energy. In all cases, the absorption coefficient reaches ~ 10^5 cm^{-1} for a photon energy of ~ 0.5eV above the absorption edge, which is typical of direct semiconductors. The curves of absorption coefficient squared are essentially linear in the range of photon energy investigated, which also implies a direct fundamental bandgap. The observed slight non-linearity of the curves for small x can be attributed to the non-parabolicity of the conduction band resulting from the $\mathbf{k}\cdot\mathbf{p}$ interaction between the Γ_6-symmetry conduction band and the Γ_8-symmetry valence bands [17].

The bandgaps determined from the absorption edges in Fig.1(b) are shown as a function of Ga concentration in Fig. 2. The absorption edge shifts rapidly to higher energy as x increases. In Ga-rich $In_{1-x}Ga_xN$ alloys, numerous studies have been done on the composition dependence of the bandgap [5-8]. In order to see the composition dependence of the bandgap in the entire composition range, two sets of previously reported data on the Ga-rich side are also shown in Fig. 2. These bandgaps were measured by photomodulated transmission (PT) [7] and optical absorption [6], respectively. It can be seen that our data on the In-rich side makes a smooth transition to the data points on the Ga-rich side. This result further confirms that the absorption edge of InN observed near 0.77 eV indeed corresponds to the intrinsic fundamental bandgap of InN [15-16]. As shown by the solid curve in Fig.2, the composition dependence of the room-temperature bandgap in the entire composition range can be well fit by the following standard equation,

$$E_G(x) = 3.42\,x + 0.77\,(1-x) - 1.43\,x\,(1-x). \qquad (1)$$

with a constant bowing parameter of b = 1.43 eV. This value of b is much smaller than previously reported bowing coefficients for which a bandgap of ~ 1.9 eV for InN was used as the lower-energy end point [5-6], and is similar to that observed (1.3 eV) in the $Al_xGa_{1-x}N$ alloy system [18]. For example, for the two sets of data points on the Ga-rich side shown in Fig. 2, if an InN bandgap of 1.9 eV is assumed instead of 0.77 eV, a bowing coefficient as large as 2.63 eV is needed to accommodate the composition dependence on the Ga-rich side. This fit is shown as a dashed curve in Fig.2. This artificial large bowing effect has also been discussed in terms of a composition dependent bowing parameter [19-20]. It has been pointed out in Ref.[6] that the variety of experimental bandgaps on the Ga-rich side can be better fit with a pseudo-linear composition dependence. Our results show that this pseudo-linear composition dependence on the Ga-rich side is just the direct evidence of the small bowing in the entire composition range. An additional significance of Fig. 2 is that it demonstrates that the fundamental bandgap of this ternary alloy system alone covers a wide spectral region ranging from near infrared at ~ 1.6 μm to near ultra-violet at ~ 0.36 μm.

The composition dependence of the peak energy of the PL signal is also shown in Fig. 2. At higher Ga concentrations, the PL peak energy is shifted towards lower energy

as compared with the absorption edge. The observed Stokes shift increases with increasing Ga content and is as large as 0.56 eV for x = 0.5. In the inset of Fig. 2, the PL peak energy is plotted as a function of absorption edge energy. Also shown in solid line is a linear fit to experimental data on the Ga-rich side [8]. The deviation from the linear interpolation (dashed line) represents the Stokes shift. It is clearly seen that the Stokes shift tends to reach the maximum near the middle of the composition, indicating inhomogeneous distribution of In and Ga atoms. The emission spectrum measured by PL spectroscopy reflects the distribution of localized states in smaller-gap regions that have larger-than-average In compositions [19, 21], while the absorption transition largely reflects the onset of the density of delocalized states. Therefore, the fact that the Stokes shift reaches the maximum around the middle of composition implies that the largest degree of composition fluctuation and/or structural disorder occurs near the middle. This is also consistent with the result that the linewidth of the PL signal increases with increasing Ga concentration, as is seen in Fig. 1(a). As discussed in Ref.[7], the PL linewidths of over 50 meV in $In_{1-x}Ga_xN$ cannot be explained by pure statistical randomness in the alloy composition without considering carrier localization caused by compositional inhomogeneity.

This carrier localization effect can also be seen from the temperature dependence of the PL signals. Fig. 2 shows the PL peak energy measured at room temperature and 11K. At low Ga concentrations, the low-temperature PL peak energy is lower than the room temperature one (by ~60meV at x = 0). As the Ga fraction increases, the difference is reduced and finally the low-temperature PL signal peaks at higher energy for large x. To understand the temperature behavior of these alloys, we have measured the PL signal of two samples over a wide temperature range (11K to 295K). The peak energy and the full width at half maximum (FWHM) are plotted as a function of temperature in Fig. 3. Both samples exhibit an anomalous temperature behavior: while the PL peak energy of InN monotonically increases as a function of temperature, a so-called inverted "S" shaped dependence is observed for $In_{0.89}Ga_{0.11}N$. This inverted S-shaped phenomenon has been observed previously in alloys such as GaInP [22], AlInAs [23], and Ga-rich InGaN [24], and in InGaN/GaN quantum wells [25], and is attributed to carrier localization. The FWHM of the PL of $In_{0.89}Ga_{0.11}N$ shows a rapid increase below the temperature (~75K)

where the bandgap minimum occurs in the S-shaped curve. Afterwards, the FWHM stays essentially constant. Below 75K, the carrier recombination is dominated by radiative process, in which the carrier lifetime increases with increasing temperature. The photo-generated carriers have more chance to relax down to the localized lower-energy states before recombining. The emission peak thus redshifts, and also significantly broadened on the lower energy side (raw data not shown here). Above 75K, non-radiative recombination becomes dominant. The carrier lifetime decreases as temperature increases and as a result, the carriers quickly recombine before relaxing down to the lower-energy tail states. Therefore, the emission peak shifts to higher energy, until the trend is compensated by the temperature-induced bandgap shrinkage. The changes in the kinetics of the emission process are thus responsible for the anomalous temperature behavior of the PL. The temperature dependence of the emission rate from the localized states can also contribute to the behavior of the photoluminescence. The monotonic increase in the PL energy of InN with increasing temperature can be understood in terms of an emission rate containing a Boltzmann factor.

In summary, we have demonstrated that In-rich $In_{1-x}Ga_xN$ alloys with $x<0.5$ have small fundamental bandgap energies ranging from around 0.77 eV to 1.75 eV. Strong infrared PL signals have been observed from these alloys. The composition dependence of the bandgap can be well explained by a relatively small bowing parameter. The Stokes shift increases with increasing Ga concentration for the compositions investigated, suggesting spatial variation of the alloy composition and strong carrier localization in the samples.

The work at the Lawrence Berkeley National Laboratory is supported by the Director, Office of Science, Office of Basic Energy Sciences, Division of Materials Sciences and Engineering of the U.S. Department of Energy under Contract No. DE-AC03-76SF00098. The work at Cornell University is supported by ONR under Contract No. N000149910936.

REFERENCES

[1] S. Nakamura, J. Vac. Sci. Technol. **A 13**, 705 (1995).

[2] I. Akasaki, S. Sota, H. Sakai, T. Tanaka, M. Koike and H. Amano, Electron. Lett. **32**, 1105 (1996).

[3] K. Itaya, M. Onomura, J. Nishio, L. Sugiura, S. Saito, M. Suzuki, J. Rennie, S. Y. Nunoue, M. Yamamoto, H. Fujimoto, Y. Kokubun, Y. Ohba, G. I. Hatakoshi and M. Ishikawa, Jpn. J. Appl. Phys., Part 2, **35**, L1315 (1996).

[4] S. Nakamura, M. Senoh, S. Nagahama, N. Iwasa, T. Yamada, T. Matsushita, Y. Sugimoto and H. Kiyoku, Appl. Phys. Lett. **70**, 1417 (1997).

[5] K. P. O'Donnell, R. W. Martin, C. Trager-Cowan, M. E. White, K. Esona, C. Deatcher, P.G. Middleton, K. Jacobs, W. van der Stricht, C. Merlet, B. Gil, A. Vantomme and J. F. W. Mosselmans, Materials Science & Engineering **B 82**, 194(2001).

[6]S. Pereira, M. R. Correia, T. Monteiro, E. Pereira, E. Alves, A. D. Sequeira and N. Franco, Appl. Phys. Lett. **78**, 2137 (2001).

[7] W. Shan, W. Walukiewicz, E. E. Haller, B. D. Little, J. J. Song, M. D. McCluskey, N. M. Johnson, Z. C. Feng, M. Schurman and R. A. Stall, J. App. Phys., **84**, 4452 (1998).

[8] K. P. O'Donnell, R. W. Martin, S. Pereira, A. Bangura, M. E. White, W. van der Stricht and K. Jacobs, Phys. Stat. Sol. (**b**) **216**, 141 (1999).

[9] V. A. Tygai, A. M. Evstigneev, A. N. Krasiko, A. F. Andreeva, and V. Ya. Malakhov, Sov. Phys. Semicond., **11**, 1257 (1977)

[10] T. L. Tansley and C. P. Foley, J. Appl. Phys., **59**, 3241 (1986)

[11] Q. Guo and A. Yoshida, Jpn. J. Appl. Phys. **33**, 2453 (1994)

[12] D. C. Look, H. Lu, W. J. Schaff, J. Jasinski, and Z. Liliental Weber, Appl. Phys. Lett., **80**, 258 (2002)

[13] H. Lu, W. J. Schaff, J. Hwang, H. Wu, G. Koley and L. F. Eastman, Appl. Phys. Lett., **79**, 1489(2001)

[14] T. Inushima, V. V. Mamutin, V. A. Vekshin, S. V. Ivanov, T. Sakon, M. Motokawa, and S. Ohoya, J. Crystal Growth, **227-228**, 481 (2001)

[15] V. Yu. Davydov, A. A. Klochikhin, R. P. Seisyan, V. V. Emtsev, S. V. Ivanov, F. Bechstedt, J. Furthmuller, H. Harima, A. V. Mudryi, J. Aderhold, O. Semchinova, and J. Graul, phys. Stat. solidi (**b**), **229**, R1 (2002)

[16] J. Wu, W W. Walukiewicz, K.M. Yu, J.W. Ager III, E.E. Haller, Hai Lu, William J. Schaff, Yoshiki Saito and Yasushi Nanishi, Appl. Phys. Lett., ID 015222APL, in press.

[17] Evan O. Kane, J. Phys. Chem. Solids. **1**, 249 (1957).

[18] W. Shan, J. W. Ager III, K. M. Yu, W. Walukiewicz, E. E. Haller, M. C. Martin, W. R. McKinney and W. Yang, J. Appl. Phys. **85**, 8505 (1999).

[19] M. Ferhat, J. Furthmuller and F. Bechstedt, Appl. Phys. Lett. **80**, 1394 (2002).

[20] P. Perlin, I. Gorczyca, T. Suski, P. Wisniewski, S. Lepkowski, N. E. Christensen, A. Svane, M. Hansen, S. P. DenBaars, B. Damilano, N. Grandjean and J. Massies, Phys. Rev. **B 64**, 115319 (2001).

[21] R. W. Martin, P. G. Middleton, K. P. O'Donnell and W. van der Stricht, Appl. Phys. Lett., **74**, 263 (1999)

[22] F. A. J. M. Driessen, G. J. Bauhuis, S. M. Olsthoorn and L. J. Giling, Phys. Rev. **B 48**, 7889 (1993)

[23] S. F. Yoon, Y. B. Miao, K. Radhakkrishnan and H. L. Duan, J. Appl. Phys. **78**, 1821 (1995).

[24] F. B. Naranjo, M. A. Sanchez-Garcia, F. Calle, E. Calleja, B. Jenichen and K. H. Ploog, Appl. Phys. Lett., **80**, 231 (2002).

[25] Yong-Hon Cho, G. H. Gainer, A. J. Fischer, J. J. Song, S. Keller, U. K. Mishra and S. P. DenBaars, Appl. Phys. Lett. **73**, 1370(1998).

FIGURE CAPTIONS

Fig.1 (a) PL signal taken at room temperature (solid line) and 11K (dashed line) for samples with Ga atomic fraction x ranging from 0 to 50%. All curves are normalized to equal height and offset vertically for clarity. (b) Room-temperature absorption coefficient squared as a function of photon energy.

Fig.2 PL peak energy and bandgap determined by optical absorption as a function of composition. Some previously reported data on the Ga-rich side are also shown (Ref.[6] and Ref.[7]). All data are taken at room temperature unless otherwise noted. The solid curve shows the fit to the bandgap energies (abs and PT) using a bowing parameter b = 1.43 eV. The dashed curve is the fit to the bandgap energies on the Ga-rich side assuming a bandgap of 1.9 eV for InN. Inset: PL peak energy plotted against absorption edge energy. The solid line is a least-square fit to experimental data on the Ga-rich side adopted from Ref.[8]. The dashed straight line shows the relation when the Stokes shift is zero.

Fig. 3 Temperature dependencies of PL peak energy and FWHM for InN and $In_{0.89}Ga_{0.11}N$.

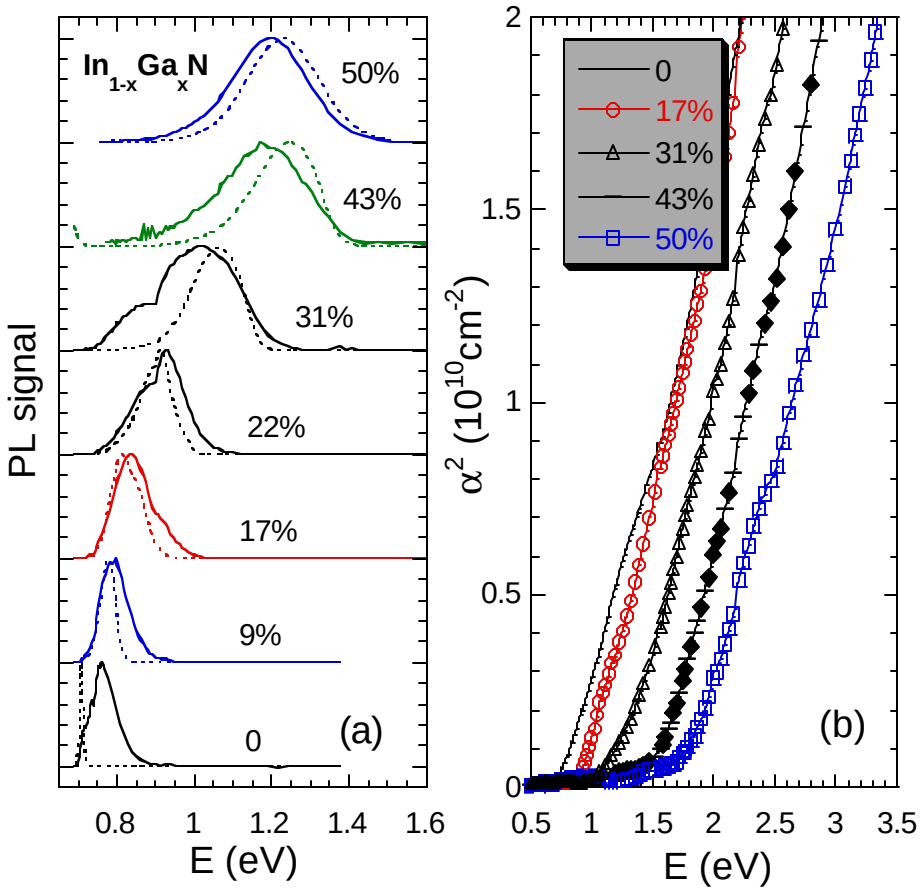
In1-xGaxN
50%
43%
31%
22%
17%
9%
0
(a)
PL signal
0.8
1
1.2
1.4
1.6
E (eV)
0
17%
31%
43%
50%
α2 (1010cm-2)
2
1.5
1
0.5
0
(b)
0.5
1
1.5
2
2.5
3
3.5
E (eV)

Fig. 1
Wu et. al.

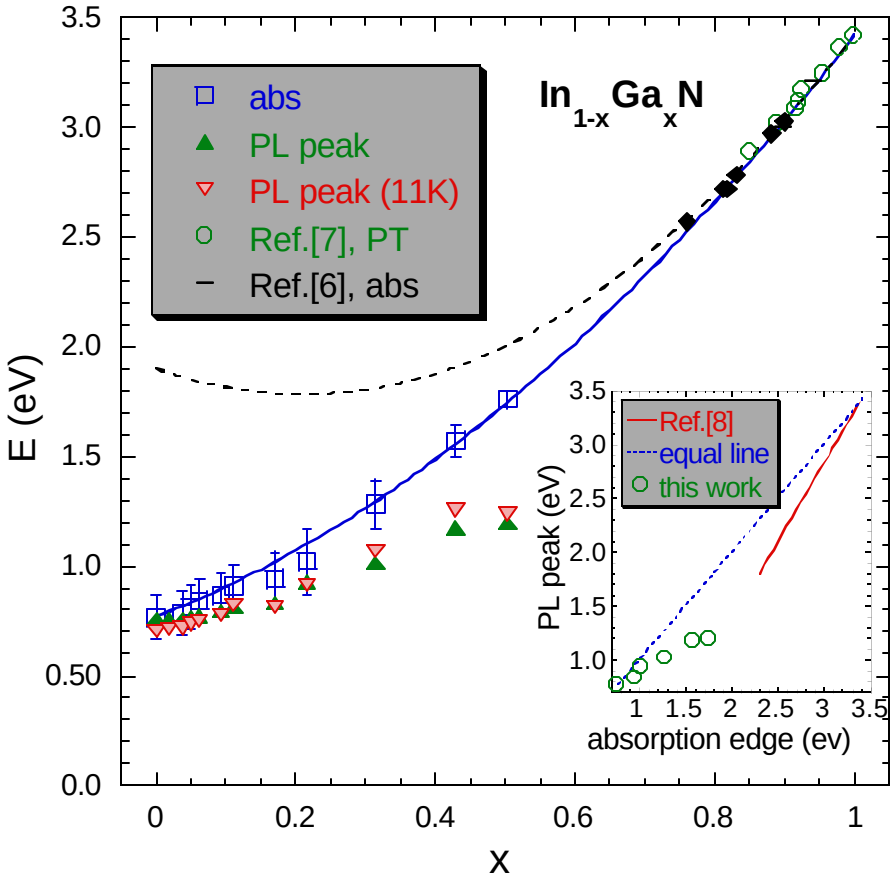
abs
PL peak
PL peak (11K)
Ref.[7], PT
Ref.[6], abs
In1-xGaxN
E (eV)
X
Ref.[8]
equal line
this work
PL peak (eV)
absorption edge (ev)

Fig. 2
Wu et. al.

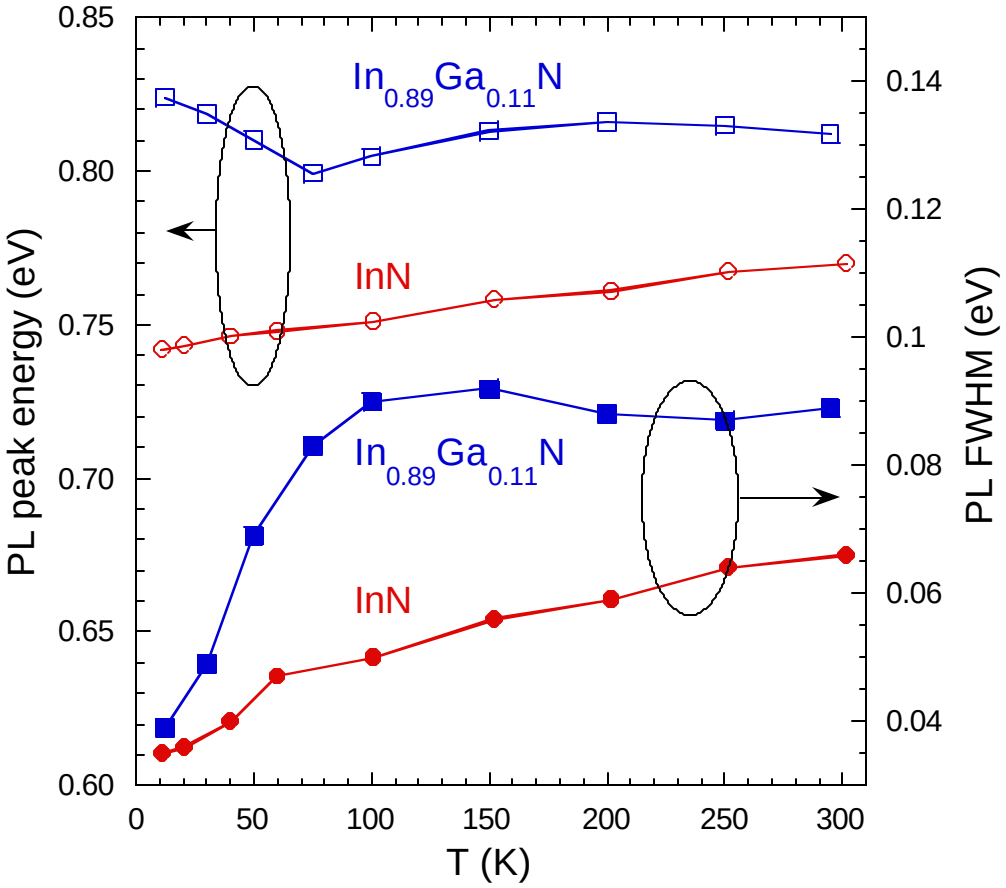
0.85
0.80
0.75
0.70
0.65
0.60
PL peak energy (eV)
0.14
0.12
0.1
0.08
0.06
0.04
PL FWHM (eV)
0
50
100
150
200
250
300
T (K)
In0.89Ga0.11N
InN
In0.89Ga0.11N
InN

Fig. 3
Wu et. al.